International Journal of Minerals, Metallurgy and Materials
Volume 22, Number 5, May 2015, Page 516
DOI: 10.1007/s12613-015-1101-3

Microstructural evolution in Al–Zn–Mg–Cu–Sc–Zr alloys during short-time homogenization

Tao Liu[1)], *Chun-nian He*[1,2)], *Gen Li*[1)], *Xin Meng*[1)], *Chun-sheng Shi*[1)], *and Nai-qin Zhao*[1,2)]

1) Department of Materials Science and Engineering, Tianjin University; Tianjin Key Laboratory of Composite and Functional Materials, Tianjin 300072, China
2) Collaborative Innovation Center of Chemical Science and Engineering, Tianjin 300072, China
(Received: 15 September 2014; revised: 27 November 2014; accepted: 1 December 2014)

Abstract: Microstructural evolution in a new kind of aluminum (Al) alloy with the chemical composition of Al–8.82Zn–2.08Mg–0.80Cu–0.31Sc–0.3Zr was investigated. It is found that the secondary phase $MgZn_2$ is completely dissolved into the matrix during a short homogenization treatment (470°C, 1 h), while the primary phase $Al_3(Sc,Zr)$ remains stable. This is due to Sc and Zr additions into the Al alloy, high Zn/Mg mass ratio, and low Cu content. The experimental findings fit well with the results calculated by the homogenization diffusion kinetics equation. The alloy shows an excellent mechanical performance after the short homogenization process followed by hot-extrusion and T6 treatment. Consequently, a good combination of low energy consumption and favorable mechanical properties is obtained.

Keywords: aluminum alloys; microstructural evolution; short-time; homogenization; grain refinement

1. Introduction

Al–Zn–Mg–Cu (7xxx series) alloys have been widely used in the aeronautical and manufacturing industries because of their high strength, sufficient stress corrosion cracking resistance (SCC), and satisfactory plasticity [1–2]. However, the disadvantages caused by the non-equilibrium phases consisting of Zn, Mg, and Cu elements, which form during casting, are also obvious; these disadvantages include a severe cracking tendency, which leads to a great reduction in strength and toughness after heat treatment and mechanical deformation, along with poor SCC resistance. In order to prevent from microsegregation and dissolve the secondary phases, homogenization heat treatment is essential. Many researchers have focused on the optimum homogenization treatment parameters [3–8]; Li *et al.* [3] claimed that the optimum temperature and duration of homogenization for Al–Zn–Mg–Cu–Sc–Zr alloys are 470°C and 24 h, respectively. Deng *et al.* [7] designed a three-stage homogenization heat treatment for Al–Zn–Mg–Cu alloys consisting of a small amount of trace Zr. However, based on these references, energy depletion and poor operation may be caused by the long holding time (12–48 h) and the complex homogenization process (more than one step) in industrial production.

Previous studies have shown that Sc and Zr are the most efficient modification agents among all microalloying additions to Al [9–12]. By adding Sc and Zr to Al alloys, the equiaxed grains and uniformly distributed second phase particles will form in the as-cast alloy rather than as long dendrites [13–17]. Consequently, both the diffusion distance of the alloying elements and the homogenization treatment period can be shortened, which is beneficial for increasing the efficiency and reducing the energy consumption.

In this work, the microstructural evolution of an Al–Zn–Mg–Cu–Sc–Zr alloy during homogenization was studied. It is found that after a short homogenization treatment, the alloy reaches a homogeneous state. The observed findings fit well with the results of the homogenization diffusion kinetic equation.

2. Materials and methods

A semi-continuous ingot with the diameter of 60 mm

Corresponding author: Nai-qin Zhao E-mail: nqzhao@tju.edu.cn

used in this work was provided by Hunan Rare Earth Metal Material Institute. The composition of the alloy was Al–8.82Zn–2.08Mg–0.80Cu–0.31Sc–0.3Zr (in wt%).

The optimal homogenization temperature was selected according to differential scanning calorimetry (DSC) analysis (STA449F3). The samples were heated in an inert atmosphere of flowing argon (Ar) at a constant heating rate of 10°C/min from 25 to 700°C, and Al_2O_3 was used as the standard sample. The specimens were homogenized at 470°C for different durations (1, 2, 12, and 16 h) in a resistance furnace (SX-G02103, the precision of temperature is ±1°C) and then quenched in water. After homogenization, the ingot was cut into a bulk with the dimensions of ϕ20 mm × 15 mm and then hot-extruded at 450°C into bars with the diameter of 5 mm. T6 treatment was performed on the obtained bars by solution treating the samples at 470°C for 1.5 h followed by water quenching. They were then aged at 120°C for 15 h. Tensile tests were performed using an electronic universal testing machine (CSS-44100) at a loading speed of 1 mm/min. The yield strengths of the samples were identified at the 0.2% plastic strain.

X-ray diffraction (XRD; Bruker D8 advanced) with Cu-K_α radiation was selected to analyze the phases in the as-cast and as-homogenized samples. Scanning electron microscopy (SEM; Hitachi S-4800 and SU1510) and energy dispersive spectroscopy (EDS) were used for microstructural observation and analysis.

3. Results and discussion

3.1. Microstructural characteristics of the as-cast ingot

The microstructure of the as-cast alloy is shown in Fig. 1. Equiaxed grains and massive secondary phases are observed. The average grain size is 38.77 μm (Fig. 1(a)). Two types of secondary phases labeled as phase A and phase B are observed with a net-like shape at grain boundaries and with a square or star-like shape within grains, respectively (Figs. 1(b)–(d)).

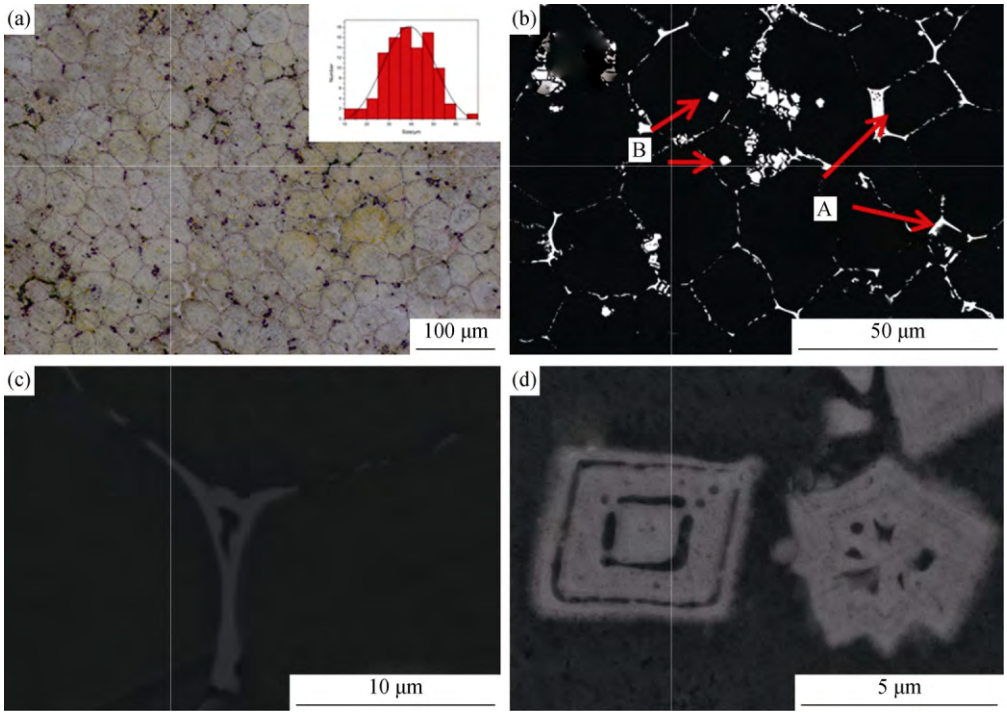

Fig. 1. Microstructures of the as-cast ingot: (a) optical microscopy image; (b) back-Scattered electron image; (c) eutectic structures; (d) primary Al_3(Sc,Zr).

In order to reveal the chemical composition of phases A and B, EDS analyses were carried out, and the results are summarized in Table 1. Phase A was enriched in Zn and Mg, whereas phase B primarily contained Sc and Zr. In addition, the amounts of Zn, Mg, and Cu were much lower in phase B than in phase A.

As shown in Fig. 2, only the $MgZn_2$ phase is present in the as-cast alloy sample, which corresponds to phase A. The EDS results (Table 1) indicate the presence of a small amount of copper in the intermetallic phase; it can be deduced that copper is dissolved into the $MgZn_2$ phase, and no phase enriched in copper will form. A previous study [18]

confirmed that the square phase (Phase B) was primary $Al_3(Sc,Zr)$ formed in the solidification process. The structure of the primary $Al_3(Sc,Zr)$ phase is considered to be cubic with the lattice parameter a = 0.410 nm, which is close to that of pure Al (a = 0.405 nm). The primary $Al_3(Sc, Zr)$ phase is an effective substrate for α-Al nucleation, leading to grain refinement and eliminating segregation and dendrite formation [11]. The addition of Mg, Zn, and Cu to the alloy enlarges the α-Al lattice parameter and reduces the mismatch between the $Al_3(Sc,Zr)$ phase and the Al matrix. The similar crystal structures of the $Al_3(Sc,Zr)$ phase and α-Al make it difficult to distinguish between their XRD patterns (Fig. 2).

Table 1. Chemical composition of the secondary phases in Fig. 1 at%

Phase	Al	Zn	Mg	Cu	Sc	Zr
A	43.49	29.05	22.54	4.40	0.37	0.15
B	78.42	2.75	0.79	1.28	7.51	9.24

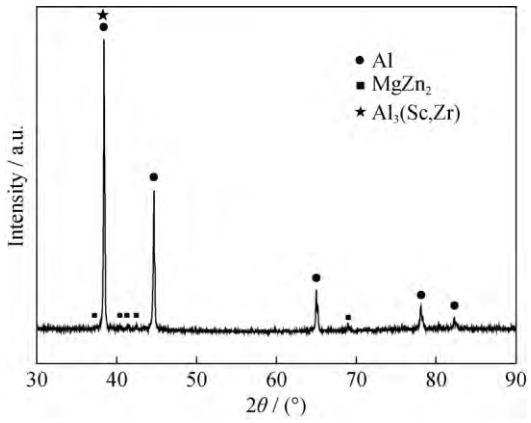

Fig. 2. XRD pattern of the as-cast alloy.

Coarse $MgZn_2$ phases in grain boundaries and compositional segregation are harmful to the subsequent deformation process; therefore, homogenization is required to prevent from severe segregation and dissolve the coarse phases into the as-cast alloy. DSC analysis was used to select a temperature for homogenization treatment. Fig. 3 shows the DSC curve of the as-cast alloy. Two obvious endothermic peaks at 472.5 and 614.7°C correspond to the melting points of non-equilibrium phases and the Al matrix, respectively. According to Røyset and Ryum [19], the melting point of $Al_3(Sc,Zr)$ is about 1320°C, which is not within the range of DSC analysis in this study (Fig. 3). To avoid over-burning, the homogenization temperature should not exceed 472.5°C. Accordingly, the homogenization temperature was selected as 470°C in this study.

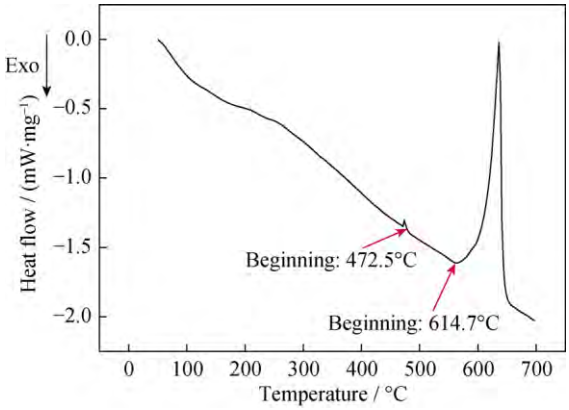

Fig. 3. DSC curve of the as-cast alloy.

3.2. Effect of homogenization on the microstructure and properties of the alloy

3.2.1. Effect of homogenization time on alloy microstructure

Fig. 4 shows the XRD patterns of the as-cast alloy and the alloys homogenized at 470°C for 1, 2, 12, and 16 h. Combining with the DSC results (Fig. 3) in which only one endothermic peak is observed within the range from 300 to 500°C, it is clear that two main phases, α-Al phase and $MgZn_2$, are present in the as-cast alloy. The diffraction peaks of the $MgZn_2$ phase disappeared after 1 h of homogenization treatment. This is due to the fact that most of the $MgZn_2$ phase was dissolved into the matrix during homogenization, resulting in a residual $MgZn_2$ content too low (lower than 5wt%) to be detected by XRD. When the homogenization time was prolonged, the peaks of the Al matrix and $Al_3(Sc,Zr)$ remained unchanged, and no other new peaks appeared.

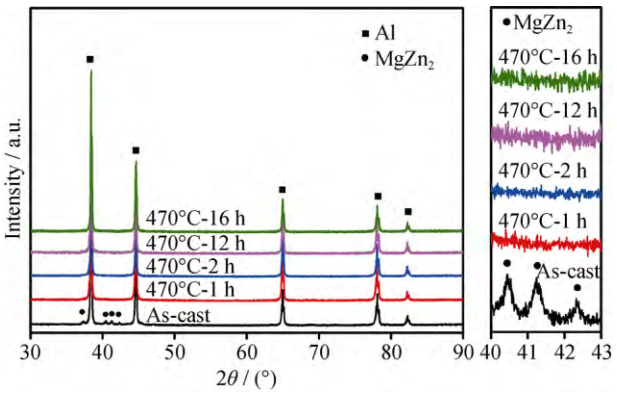

Fig. 4. XRD patterns of the as-cast specimens at different homogenization conditions.

The DSC curves of the alloys homogenized for different times are shown in Fig. 5. Compared with Fig. 3, the endothermic peak at 472.5°C disappeared from the curves of the alloys homogenized for 1 h or longer (2 and 4 h). In addition, no obvious DSC peak appeared in the curves of the as-ho-

mogenized alloys, with the exception of the Al melting point peak. These results suggest that the $MgZn_2$ phases are fully decomposed and dissolved into the matrix after a short period of homogenization (1 h).

Fig. 6 presents the SEM images and EDS maps of the as-cast alloy and the alloy homogenized at 470°C for 1 h. The secondary phases (Fig.1(c)) are rich in Zn and Mg but poor in Cu because the Cu content is 0.8 wt%. The segregation degree of Cu is weaker than those of Zn and Mg. The aggregation of Sc and Zr occurs where the square-shaped primary Al_3(Sc, Zr) phase is located. In the sample homogenized at 470°C for 1 h (Fig. 6(b)), Zn, Mg, and Cu are evenly distributed in the matrix, but the primary Al_3(Sc,Zr) phase still remains because it is too stable to decompose.

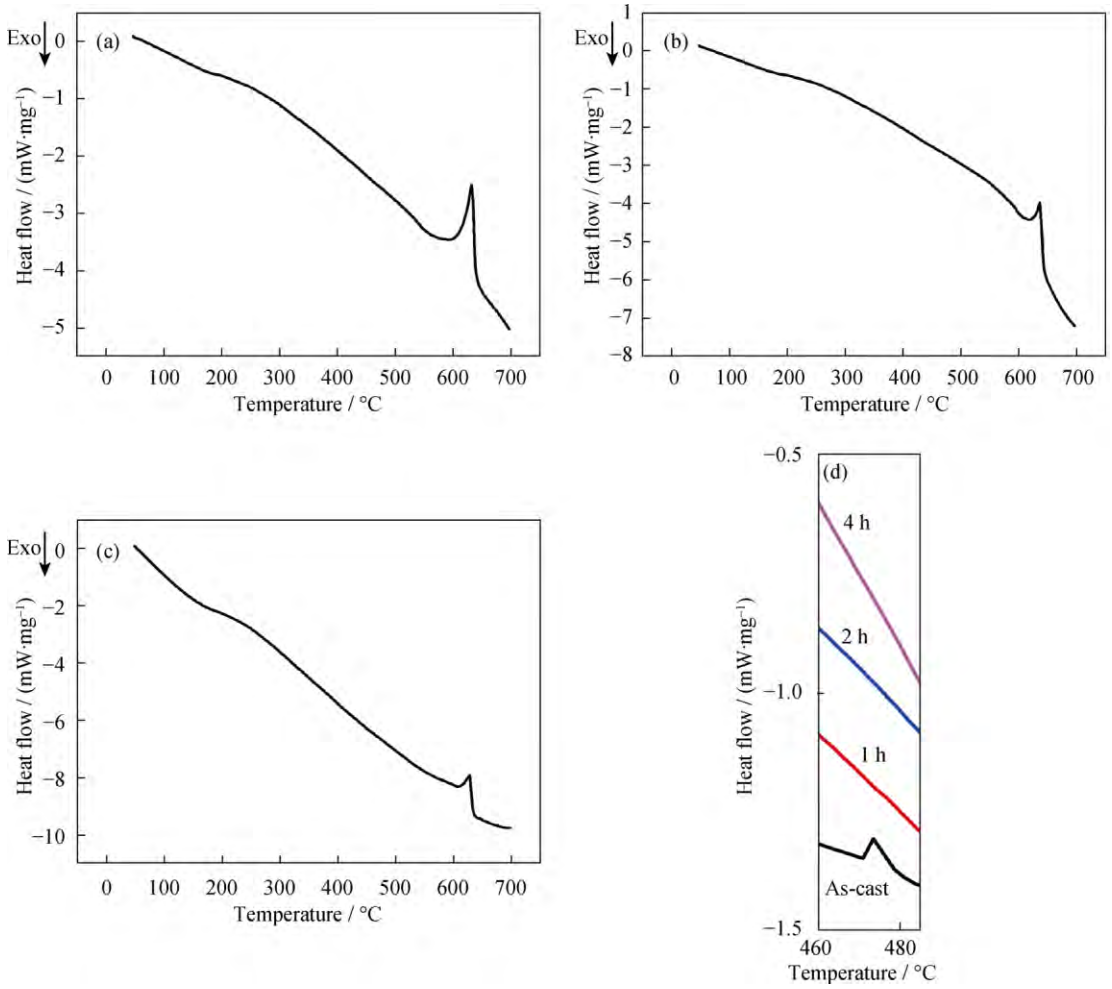

Fig. 5. DSC curves of the as-homogenized alloys: (a) 470°C, 1 h; (b) 470°C, 2 h; (c) 470°C, 4 h; (d) comparison of the above curves within the range from 460°C to 480°C.

Previous reports [5,20] have illustrated that there are four kinds of intermetallic phases in the Al–Zn–Mg–Cu alloy: $MgZn_2$, T(AlZnMgCu), S(Al_2MgCu), and θ(Al_2Cu). The formation of these phases is highly dependent on alloy composition. For example, when the elemental Cu content is less than 1.0wt%, Cu exists as a solute in the alloy rather than forming another Cu-enriched phase [21]. In the present work, the content of Cu is 0.8wt% (<1.0wt%); thus, the formation of the θ(Al_2Cu) phase is impossible. Furthermore, the contents of Zn and Mg may determine the types of Zn-containing phases formed in the as-cast alloy. It is understood that when the Zn/Mg ratio is larger than 2.2, there is a tendency to form $MgZn_2$ rather than S or T phases in the as-cast alloy [22–23]. The alloy used in this study has a high content of Zn(8.82wt%), a low content of Cu(0.8wt%), and a high Zn/Mg mass ratio (4.2); therefore, it is entirely possible that only one kind of secondary phase ($MgZn_2$ containing Cu and Al) is present in the as-cast alloy. Previous studies have reported that Al and Cu can be dissolved into the $MgZn_2$ phase to form $Mg(Zn,Cu,Al)_2$ [21,24]. However, according to Table 1, the content of Cu in the $MgZn_2$ phase is only 4.4at%, which is much lower than the contents

of Zn (22.95 at%) and Mg (22.54 at%). Meanwhile, the atomic ratio of the secondary phase ($MgZn_2$) in this work does not match that of $Mg(Zn,Cu,Al)_2$; thus, it is deduced that the effect of Cu on alloy segregation is smaller than the effects of Zn and Mg. In addition, the diffusion of Zn and Mg in the alloy significantly influences the alloy homogenization process. The eutectic phases ($MgZn_2$) decompose quickly during homogenization; however, the dissolution rates of the T and S phases are rather slow. Thus, the $MgZn_2$ phases can be dissolved into α-Al and the alloy to produce a homogeneous state after a short period of homogenization.

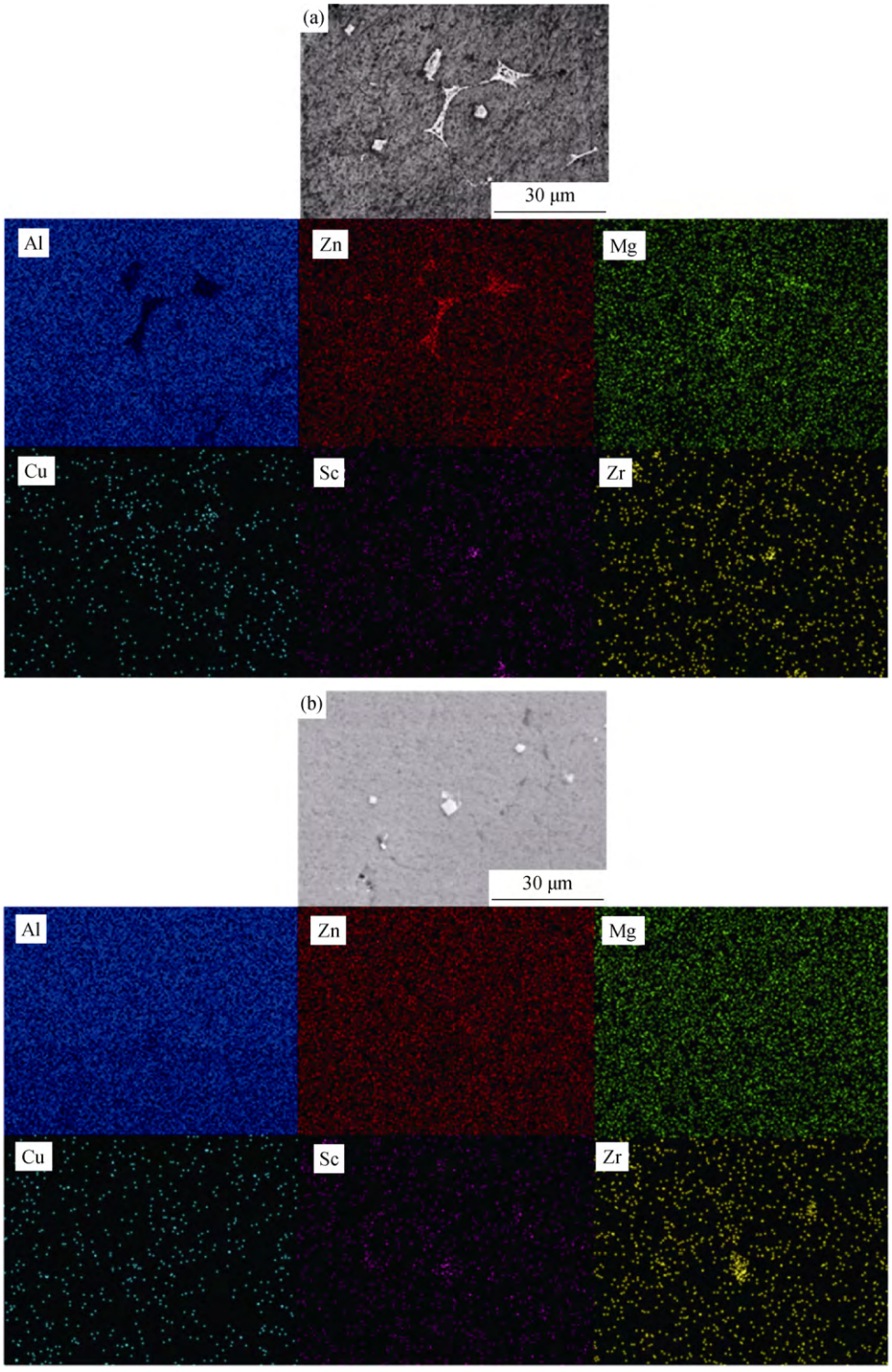

Fig. 6. EDS maps of the as-cast alloy (a) and the alloy homogenized for 1 h (b).

The primary $Al_3(Sc,Zr)$ phase is considered as a stable phase that could hardly decompose during heat treatment, even prolonging the holding time [19]. Although the primary $Al_3(Sc,Zr)$ phase plays a crucial role in refining the grains, it may cause disadvantages during the subsequent deforming procedure due to the formation and growth of cracks at the interface between the primary $Al_3(Sc,Zr)$ and the Al matrix. Therefore, it is necessary to control the size and distribution of the primary $Al_3(Sc,Zr)$ during the casting process.

3.2.2. Homogenization kinetics analysis

The variation in the concentrations of alloy components during the homogenization process can be described by Fick's law of diffusion. According to Deng *et al.* [20] and Wang *et al.* [24], the homogenization diffusion kinetic equation is given as follows:

$$\exp\left[-\frac{4\pi^2 D_0 t}{L^2}\exp\left(-\frac{Q}{RT}\right)\right]=\frac{1}{100} \quad (1)$$

where T, t, and Q are the homogenization temperature, homogenization time, and activation energy of element diffusion, respectively, L is the diffusion distance of solute atoms, which is the average grain size in this work, and D_0 is the diffusion coefficient of the element that controls the homogenization process. As reported by Wang *et al.* [24], the homogenization process is believed to be controlled by Cu diffusion due to its low diffusion coefficient ($D_{Cu} < D_{Mg} < D_{Zn}$); however, in his work, there exists a myriad of secondary phases with high Cu content in the alloy, including the S and T phases. As mentioned above, the segregation of Cu is weaker compared to those of Zn and Mg, and there is no Cu-enriched phase in the alloy. Thus, it is deduced that the homogenization process in the present study is mainly controlled by Mg diffusion.

By substituting $D_{0(Mg)} = 1.2 \times 10^{-4}$ m^2/s, $Q_{diff(Mg)} = 131$ kJ/mol, and $R = 8.314$ J/(mol·K) into Eq.(1), the homogenization kinetics curves of the alloys with different grain sizes are obtained (Fig. 7). These curves indicate that the homogenization time drops significantly with increasing homogenization temperature and decreasing grain size, especially when the temperature exceeds 450°C. Therefore, there are two ways to shorten the homogenization time: (1) by improving the homogenization temperature; and (2) by minimizing the grain size. Taking the overburning caused by high temperature into consideration, the most efficient method to minimize the homogenization time is to refine the grain size.

In this work, at a homogenization temperature of 470°C and a grain size of 38.77 μm, the theoretical holding time was 0.65 h, which is consistent with the experimental result (1 h).

3.3. Study on mechanical properties

After homogenization for 1 h, the alloy was hot extruded at 450°C, and tensile testing was then conducted. The results show that this process produces an alloy with acceptable properties: $\sigma_b = 546$ MPa, $\sigma_s = 398$ MPa, and $\delta = 9.5\%$. Fig. 8 shows the fracture microstructure of the extruded sample. Its fracture surface consists of a mass of uniformly distributed dimples with small sizes (approximately 1 μm). This result implies that the alloy is homogenous, and few coarse secondary phases exist in the dimples after the short homogenization treatment.

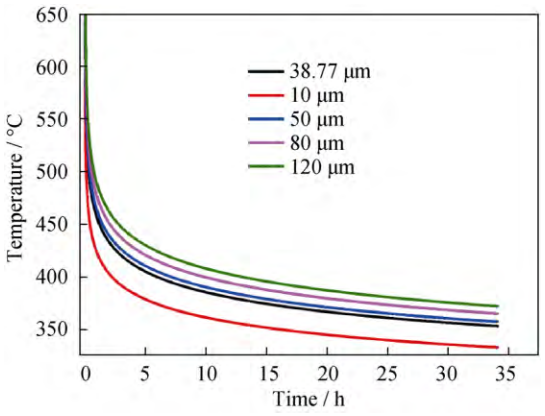

Fig. 7. Homogenization kinetics curves.

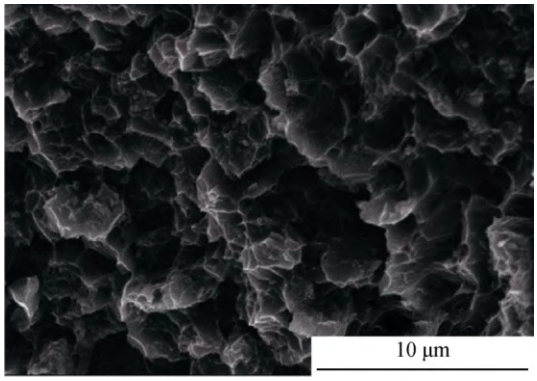

Fig. 8. SEM micrograph of the extruded alloy.

Table 2 shows the mechanical properties of the sample homogenized for 1 h followed by T6 treatment; the results of previous studies regarding different homogenization times are also listed for comparison. In this work, both high strength and elongation were achieved after solution-aging treatment (Table 2; $\sigma_b = 746.9$ MPa, $\sigma_s = 720.7$ MPa, and $\delta = 10.9\%$). The strength of the alloy (T6) is obviously improved compared with that of the extruded sample due to the large number of precipitated phases formed during the aging

process. A high level of solubility of Mg, Zn, and Cu can be obtained via a short homogenization treatment due to grain refinement, enhancing the kinetics of aging precipitation. Consequently, the alloy possesses excellent mechanical properties after a short homogenization and T6 treatment compared with those subjected to long homogenization processes.

The results demonstrate that the new short homogenization heat treatment generates a good balance between the low energy expenditure and the super-high alloy mechanical performance.

Table 2. Mechanical performances of alloys homogenized for different time

Composition	Homogenization time / h	Tensile strength / MPa	Yield strength / MPa	Elongation / %
Al–8.82Zn–2.08Mg–0.80Cu–0.31Sc–0.3Zr	1 (this work)	746.9	720.7	10.9
Al–5.41Zn–1.98Mg–0.33Cu–0.25Sc–0.1Zr	12 [17]	555	524	12.3
Al–6.1Zn–2.1Mg–0.12Sc–0.14Zr	24 [6]	535	515	11
Al–7.05Zn–2.35Mg–1.55Cu–0.49Sc–0.14Zr	48 [25]	600	505	12

4. Conclusions

(1) Equiaxed grains and massive secondary phases, primary $Al_3(Sc,Zr)$ and $MgZn_2$, are obtained in the as-cast alloy with the composition of Al–8.82Zn–2.08Mg–0.80Cu–0.31Sc–0.3Zr (in wt%).

(2) The Al–Zn–Mg–Cu–Sc–Zr alloy reaches a homogenous state after a short homogenization treatment (470°C, 1 h), which agrees with the results of the homogenization kinetics equation.

(3) An excellent combination of outstanding mechanical properties and high energy efficiency is achieved by the new short-time homogenization heat treatment.

Acknowledgements

This work was financially supported by the High Technology Research and Development Program of China (No. 2013AA031002).

References

[1] H.A. Godinho, A.L.R. Beletati, E.J. Giordano, and C. Bolfarini, Microstructure and mechanical properties of a spray formed and extruded AA7050 recycled alloy, *J. Alloys Compd.*, 586(2014), No. S1, p. S139.

[2] Ł. Rogal, J. Dutkiewicz, H. Atkinson, L. Lityńska-Dobrzyńska, T. Czeppe, and M. Modigell, Characterization of semi-solid processing of aluminium alloy 7075 with Sc and Zr additions, *Mater. Sci. Eng. A*, 580(2013), p. 362.

[3] W.B. Li, Q.L. Pan, Y.P. Xiao, Y.B. He, and X.Y. Liu, Microstructural evolution of ultra-high strength Al–Zn–Cu–Mg–Zr alloy containing Sc during homogenization, *Trans. Nonferrous Met. Soc. China*, 21(2011), No. 10, p. 2127.

[4] S.Y. Chen, K.H. Chen, GS. Peng, X.H. Chen, and Q.H. Ceng, Effect of heat treatment on hot deformation behavior and microstructure evolution of 7085 aluminum alloy, *J. Alloys Compd.*, 537(2012), p. 338.

[5] X.G. Fan, D.M. Jiang, Q.C. Meng, and L. Zhong, The microstructural evolution of an Al–Zn–Mg–Cu alloy during homogenization, *Mater. Lett.*, 60(2006), No. 12, p. 1475.

[6] L.M. Wu, W.H. Wang, Y.F. Hsu, and S. Trong, Effects of homogenization treatment on recrystallization behavior and dispersoid distribution in an Al–Zn–Mg–Sc–Zr alloy, *J. Alloys Compd.*, 456(2008), No. 1-2, p. 163.

[7] Y.L. Deng, Y.Y. Zhang, L. Wan, A.A. Zhu, and X.M. Zhang, Three-stage homogenization of Al–Zn–Mg–Cu alloys containing trace Zr, *Metall. Mater. Trans. A*, 44(2013), No. 6, p. 2470.

[8] H. Li, D.H. Cao, Z.X., Wang, and Z.Q. Zheng, High-pressure homogenization treatment of Al–Zn–Mg–Cu aluminum alloy, *J. Mater. Sci.*, 43(2008), No. 5, p. 1583.

[9] A.F. Norman, P.B. Prangnell, and R.S. McEwen, The solidification behaviour of dilute aluminium–scandium alloys, *Acta Mater.*, 46(1998), No. 16, p. 5715.

[10] I.G. Brodova, D.V. Bashlikov, and I.V. Polents, Influence of heat time melt treatment on the structure and the properties of rapidly solidified aluminum alloys with transition metals, *Mater. Sci. Forum*, 269-272(1998), p. 589.

[11] S. Golubev, O. Korzhavina, P. Popel, V. Kononenko, I. Brodova, I. Polents and T. Shubina, Effect of viscosity and electrical-resistance of the structural state of Al–Sc melts and the structure of the cast metal, *Russ. Metall.*, (1991), No. 1, p. 44.

[12] E.A. Marquis and D.N. Seidman, Coarsening kinetics of nanoscale Al_3Sc precipitates in an Al–Mg–Sc alloy, *Acta Mater.*, 53(2005), No. 15, p. 4259.

[13] J.D. Robson and P.B. Prangnell, Modelling Al_3Zr dispersoid precipitation in multicomponent aluminium alloys, *Mater. Sci. Eng. A*, 352(2003), No. 1-2, p. 240.

[14] N. Blake and M. Hopkins, Constitution and age hardening of Al–Sc alloys, *J. Mater. Sci.*, 20(1985), No. 8, p. 2861.

[15] M.J. Jones and F.J. Humphreys, Interaction of recrystallization and precipitation: the effect of Al_3Sc on the recrystallization behaviour of deformed aluminium, *Acta Mater.*, 51(2003), No. 8, p. 2149.

[16] D.N. Seidman, E.A. Marquis, and D.C. Dunand, Precipitation

strengthening at ambient and elevated temperatures of heat-treatable Al (Sc) alloys, *Acta Mater.*, 50(2002), No. 16, p. 4021.

[17] Y. Deng, Z.M. Yin, K. Zhao, J.Q. Duan, and Z.B. He, Effects of Sc and Zr microalloying additions on the microstructure and mechanical properties of new Al–Zn–Mg alloys, *J. Alloys Compd.*, 530(2012), p. 71.

[18] K.B. Hyde, A.F. Norman, and P.B. Prangnell, The effect of cooling rate on the morphology of primary Al_3Sc intermetallic particles in Al–Sc alloys, *Acta Mater.*, 49(2001), No. 8, p. 1327.

[19] J. Røyset and N. Ryum, Scandium in aluminium alloys, *Int. Mater. Rev.*, 50(2005), No. 1, p. 19.

[20] Y. Deng, Z.M. Yin, and F.G. Cong, Intermetallic phase evolution of 7050 aluminum alloy during homogenization, *Intermetallics*, 26(2012), p. 114.

[21] X.M. Li and J.J. Yu, Modeling the effects of Cu variations on the precipitated phases and properties of Al–Zn–Mg–Cu alloys, *J. Mater. Eng. Perform.*, 22(2013), No. 10, p. 2970.

[22] S.K. Maloney, K. Hono, I.J. Polmear, and S.P. Ringer, The chemistry of precipitates in an aged Al–2.1Zn–1.7Mg at.% alloy, *Scripta Mater.*, 41(1999),No.10, p. 1031.

[23] M. R. Clinch, S. J. Harris, W. Hepples, N. J. H. Holroyd, M. J. Lawday, and B. Noble, Influence of zinc to magnesium ratio and total solute content on the strength and toughness of 7xxx series alloys, *Mater. Sci. Forum*, 519(2006), p. 339.

[24] H.J. Wang, J. Xu, Y.L. Kang, M.G. Tang, and Z.F. Zhang, Study on inhomogeneous characteristics and optimize homogenization treatment parameter for large size DC ingots of Al–Zn–Mg–Cu alloys, *J. Alloys Compd.*, 585(2014), p. 19.

[25] O.N. Senkov, R.B. Bhat, S.V. Senkova, and J.D. Schloz, Microstructure and properties of cast ingots of Al–Zn–Mg–Cu alloys modified with Sc and Zr, *Metall. Mater. Trans. A*, 36(2005), No. 8, p. 2115.